Vol. 22, No. 2 (2021) 294-309, DOI: 10.24874/ti.1165.08.21.11

Tribology in Industry

www.tribology.rs

RESEARCH

Investigation on the Mechanical and Wear Behaviour of Al-6082-BN-B_4C-Corn Cob Ash Hybrid Composites

Manu Sam[a], N. Radhika[a,*], Valluri Sidvilash[a], T. Mohanraj[a]

[a]*Department of Mechanical Engineering, Amrita School of Engineering, Coimbatore, Amrita Vishwa Vidyapeetham, India.*

Keywords:

Aluminum Metal Matrix Composites
Stir casting
Wear rate
Wear resistance

* Corresponding author:

N. Radhika
E-mail: n_radhika1@cb.amrita.edu

Received: 12 August 2021
Revised: 20 September 2021
Accepted: 11 November 2021

A B S T R A C T

This study comparatively investigates the rotational dry sliding wear behaviour of hybrid ceramic reinforced AA6082/3wt.%Boron Nitride (BN)/4wt.%Boron Carbide (B_4C) stir cast composite against its alloy by varying weight percentage (2, 4 and 6 wt.%) of Corn Cob Ash. Maximum hardness (70.7 BHN) and impact strength (32 J) was identified at 4 wt.%. The input parameters were applied load (15, 25 and 35 N), sliding distance (750, 1250, and 1750 m) and sliding velocity (1, 2 and 3 m/s), whereas specific wear rate was the response parameter designed based on Taguchi's L_{27} array. The percentage contribution of each influential input factor towards the performance characteristics of the developed composites were defined using Analysis of Variance. Optimum wear rate was obtained at 15 N load, 750 m sliding distance and 1 m/s sliding velocity combination. Signal to Noise ratio identified applied load as most influential followed by sliding distance and sliding velocity.

© 2022 Published by Faculty of Engineering

1. INTRODUCTION

The convergence of diverse industrial requirements and demand for high strength to weight ratio on products over the past decade made Aluminum Metal Matrix Composites (AMMCs) popular among industries like automobile, aviation, defense and ship industries [1]. Incorporating diverse properties within a same component or improving existing properties is achieved through reinforcing aluminium matrix with two or more reinforcements, resulting in hybrid composites [2]. Selection of matrix material, reinforcement variants, particle size and weight percentage, fabrication technique, matrix distribution and interfacial strength are few major factors that directly influence the AMMC properties [3-5].

Increasing content of natural fiber ash as a reinforcement in AMMCs, up to a limit of 10-15 wt.% reported to improve its tribo-mechanical properties [6]. Abundancy and cost effectiveness of natural fibers are increasing its popularity as a raw material for diverse sectors of engineering [7]. Effective distribution of fibrous reinforcements across the aluminium matrix is a major challenge. Stir casting is reported to be a

successful cost-effective manufacturing technique that facilitates effective distribution of fibrous reinforcements [8,9].

Agro-wastes such as ash of groundnut shell, rice husk, coconut shell, corn cob and bagasse are mostly preferred natural fiber reinforcements. This is due to the rich presence of silicon, aluminum and magnesium oxide which improve the mechanical and wear properties of the AMMC [10]. Al/Y_2O_3/rice husk composite fabricated using two-step stir casting process showed improved hardness with rise in Rusk Husk Ash (RHA) content. The rise in wear rate with respect to applied load was controlled by the presence of oxides in RHA [11]. Al7075 reinforced with Coconut Shell Ash (CSA) exhibited supreme wear resistance at higher temperature and load, due to the relative stability of incoherent high diameter particles along the grain boundary which are thermodynamically stable. These particles effectively inhibit the dislocation movement [12]. Coefficient of friction (COF) at the sliding tribo-surface was effectively controlled by the oxide presence of interfacial wear debris. Addition of fly ash (7 wt.%) and B_4C (3wt.%) in aluminium resulted in effective particle distribution and superior mechanical properties like hardness (111 BHN), Ultimate Tensile Strength (290 MPa) and % elongation (0.75 mm) [13]. Al-Si-Mg/4wt.%SiC/6wt.%Corncob hybrid composite developed through two-step stir casting process resulted in a low cost-high performance composite with superior micro-hardness, tensile strength and wear resistance with a minimum porosity of 4% [14]. Corn Cob particles (25 wt.%) and E-Glass Fibers (5 wt.%) with Epoxy as hardener in aluminium matrix resulted in a hybrid composite produced through hand layup process. This hybrid epoxy composite was identified as an alternative for synthetic fiber reinforced composite materials with an optimum impact strength of 14.06-27.16 KJ/m^2 [15] AA6061 composites produced with reinforcement combinations of 15% SiC, 5%SiC/10%FA, 5%SiC/10 Neem leaf ash (NLA) using liquid metallurgy route reported that interaction of ceramics and natural fibers in aluminium ensured improved machinability through effective distribution and reduced clustering [16]. Taguchi's method effectively predicted the contribution of input factors on wear response and identified the optimum parametric combination (Load-20 N, Velocity-4 m/s and Radial Distance from Outer Surface -15 mm) for efficient sliding wear performance of SiC/Al6061 composite [17]. A similar study on nano-Al_2O_3 and SiC reinforced hybrid AMMCs using Taguchi's statistical method identified applied load (36.94%) and sliding distance (23.82%) as most influential factors during dry sliding [18]. Allotropes of carbon in combination with aluminium-ceramic matrix triggers self-lubrication and limits friction [19].

In the present work, AA6082 alloy and its hybrid composites were synthesized via stir casting route. Scientific combination with proportional usage of ceramics (BN, B_4C) and Corn Cob Ash (CCA), intend to effectively control the tribo-mechanical performance of the developed composite. Such developed composites are tested under unlubricated condition. Few researchers have successfully attempted hybrid ceramic binary reinforcing along with stir cast aluminium composite [20-22], to improve the tribo-mechanical properties. Even though, utilization of non-ceramic 'CCA' as a tertiary reinforcement along with primary and secondary ceramics is a novel approach among stir cast aluminium hybrid composites. Therefore, this research conducts a comparative analysis to identify the best composition and statistically recommends it for superior tribo-mechanical applications for diverse industries like military, aviation and pneumatics.

2. MATERIALS AND METHOD

2.1 Alloy and reinforcements

Commercially available AA6082 alloy was procured and used as matrix for this composite. To analyze and validate the composition of AA6082 alloy, optical emission spectroscopic test was performed and the elemental details of alloy is presented in Table 1.

B_4C and BN of average size 40 μm were procured from the domestic vendors of Coimbatore, India. Whereas, the corncobs were procured in large volumes from Hyderabad, India. The corncobs were sun dried to remove moisture content. Dried corncobs were burned in open air, until complete combustion. The obtained ash was allowed to air quench at room temperature. The CCA of average size 35 μm was conditioned at 650^0C for 180 min, using an electric furnace. This technique effectively limited the carbonaceous and volatile constituent presence in the ash.

Table 1. Elemental composition of AA6082.

Elements	Weight Percentage (wt.%)
Si	0.920
Fe	0.203
Mn	0.416
Mg	0.878
Zn	0.105
Sn	0.117
Cu	0.040
Cr	0.032
Ni	0.042
Ti	0.016
Pb	0.040
Ca	0.004
Zr	0.008

Sieve shaker was used to obtain uniform size of particles. The chemical composition of the CCA [23] is shown in the Table 2.

Table 2. Chemical composition of CCA.

Constituents	Weight Percentage (wt.%)
SiO_2	77.05
Al_2O_3	5.64
FeO_3	2.97
CaO	2.45
MgO	1.71
TiO_2	0.25
Na_2O	0.49
K_2O	3.81
P_2O_3	0.71
MnO	0.23

2.2 Composite fabrication and testing

AA6082 alloy and AA6082/3wt.%BN/4wt.%B_4C hybrid composites were stir cast. Keeping 3wt.%BN and 4wt.%B_4C constant, CCA was introduced as a tertiary reinforcement varied at 2, 4, 6wt.% using stir casting technique. For maximum tribo-mechanical performance of aluminium based hybrid composites, the overall reinforcement weight percentage needs to be limited within a range of 8-12 wt.% [24]. This controls undesirable clustering and precipitations during casting [25]. Limiting the proportion of B_4C at 4wt.%, facilitates effective distribution within the matrix and avoids clustering [26]. Addition of 3 wt.% BN prevents segregation or layering phenomenon during stirring process [27,28].

The CCA, BN and B_4C were initially preheated to 250^0C for the removal of moisture and to improve the wettability [29] with AA6082 alloy melt. AA6082 ingots were melt using a graphite made crucible in an electric crucible furnace, by heating to a temperature of 700^0C (above liquids temperature of alloy) [30]. The preheated BN, B_4C and CCA along with 0.1wt.% magnesium was stirred at molten form.

Even though costly, B_4C was preferred as reinforcement with AA6082, due to its superior strength, lower density, excellent hardness and chemical resistance [31]. The density closeness with matrix facilitates homogeneous distribution with conventional stirring process. BN is popular for its excellent wettability with aluminium matrix, solid lubricating effect and load bearing ability [32]. The presence of derivatives of agro wastes in aluminium composites, control overall inventory cost, improves machinability, lowers density, and limits environmental pollution. A few researchers reported that a number of agro wastes were processed into ashes, and when used as reinforcing materials in aluminium matrix produced better properties than alloy [33].

Stir casting was identified as the most prominent and economic industrial production technique, due to its exceptional capability to facilitate uniform distribution of reinforcements and produce fine microstructures through fast cooling [34]. This can result in minimal porosity and good quality bonding at the particle-matrix interfaces. Stirring speed, stirring duration and blade angle are the most influential stirrer parameters that has direct influence over the properties of cast composites. In this research, the molten alloy was stirred at a speed of 350 rpm for a duration of 5 minutes with a blade angle of 30°, for effective distribution and thus preventing clustering phenomenon. In a similar research, optimized blade angle was identified as 30°, where minimal clustering of fly ash and homogenous distribution of B_4C was obtained in aluminium matrix [35]. The vortex formed at this angle dispenses heterogeneous reinforcement particles within the melt and produces a homogeneous distribution of heterogeneous reinforcements within the matrix [36]. A schematic representation of the stir casting setup utilized for this research is shown in Fig. 1.

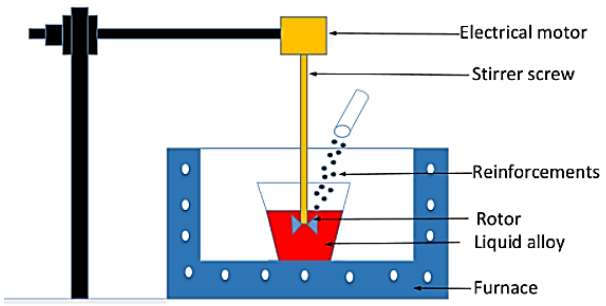

Fig. 1. Schematic setup of stir casting.

The die was preheated to 200^{0}C and molten metal was poured into the die. Preheating the die helps to reduce the thermal mismatch between the molten metal and inner surface of die. This minimizes the risk of defects like porosity, shrinkage etc [37].

Specimens from each cast sample was subjected to Brinell hardness measurement using a Brinell hardness tester(model B3000), with a ball shaped indenter of ø5 mm. Specimens were prepared for the test based on ASTM E10 standard to obtain a smooth flat surface with excellent finish. A load of 250 kgf was applied against this polished surface following standard procedures. The embossed indentation was used to calculate the material hardness. The surface polishing is performed up to an extent, where the outer curvature of indentation is clearly defined through microscope. Average values of five repeated trials on each specimen was utilized for effective comparison.

In order to analyze the impact strength and material toughness, the developed samples of each were subjected to impact test using Pantec made (Model: CHIZ-25) operational at 220 V x60 Hz. The setup consists of pendulum with 11 and 22 J hammers. The specimens for testing were prepared (dimension 62.5 × 12.7 × 10 mm) according to ASTM D256 standard with smoothly finished edges and defined 'V' notch. Impact test details the deformation behaviour of the developed material, material response to high strain rate and tri-axial stress induced at the notch zone. Impact strength is also significantly dependent over the mode of fracture of the developed material, especially for hybrid composites with particle induced ductile-brittle.

Microstructural analysis was conducted on each cast sample to detail the grain refinement and particle distribution. These samples were prepared based on ASTM E3 standard and analyzed using an inverted metallurgical microscope (Model: Zeiss Axiovert 25CA). Test specimen surface was ground to flatten and polished using emery grit grades of 80, 120, 360, 600 and 800. This surface was further micro-polished using Al_2O_3 solution against velvet cloth. Keller's reagent was used as an etchant to obtain an effective contrast of topography at high magnification.

Rotational wear performance of the developed samples were tested and compared using a pin-on-disc tribo-tester. The test samples were prepared according to ASTM G99 standard. Standard pin of sliding area - 10 × 10 mm and height – 30 mm were used to experimentally evaluate loss of volume, wear rate and specific rate of wear. Input parameters used for experimentation involved applied load (15, 25, 35 N), sliding velocity (1, 2, 3 m/s) and sliding distance (750, 1250, 1750 m).

3. RESULTS AND DISCUSSION

3.1 Microstructure

Metallography analysis was conducted on alloy and hybrid composites as shown in Figure 2. For AA6082 alloy, the analysis revealed (Fig. 2a) better grain refinement imparting superior strength. Whereas, AA6082/3wt.%BN/4wt.%B_4C hybrid composite revealed (Fig. 2b) that closeness in density of both ceramics with aluminum matrix, facilitated effective distribution of ceramics throughout the matrix. With addition of CCA, defined and coarser grains were observed (Fig. 2c) for AA6082/3wt.%BN/4wt.%B_4C/2wt.%CCA hybrid composite. Increasing the wt.% of CCA up to 4 wt.%, revealed (Fig. 2d) uniform distribution of reinforcements without clustering phenomenon and a refined granular structure. Whereas, further increment in wt.% of CCA in AA6082/3wt.%BN/4wt.%B_4C/6wt.%CCA hybrid composite resulted in meagre clustering and uneven particle distribution as shown in Fig. 2e.

Uniform dispersion of particles within the matrix plays a vital role in improving the composite properties. Such particle positioning within the matrix, forms effective strengthening mechanisms like dislocations bowing/Orowan looping around the reinforcement particles. Incorporation of diverse hard particles (B_4C and BN) into Al

matrix, act as a barrier that hinders the crack propagation with increase in dislocation density. The density closeness of these particles along with aluminium matrix prevents segregation and particle settling phenomena during stirring, promoting uniform distribution. Dispersion of such particles create loops, leading to decrement in mean spacing within the adjacent particles. The induction of local hydrodynamic forces restricts further dislocation and thereby improves strength.

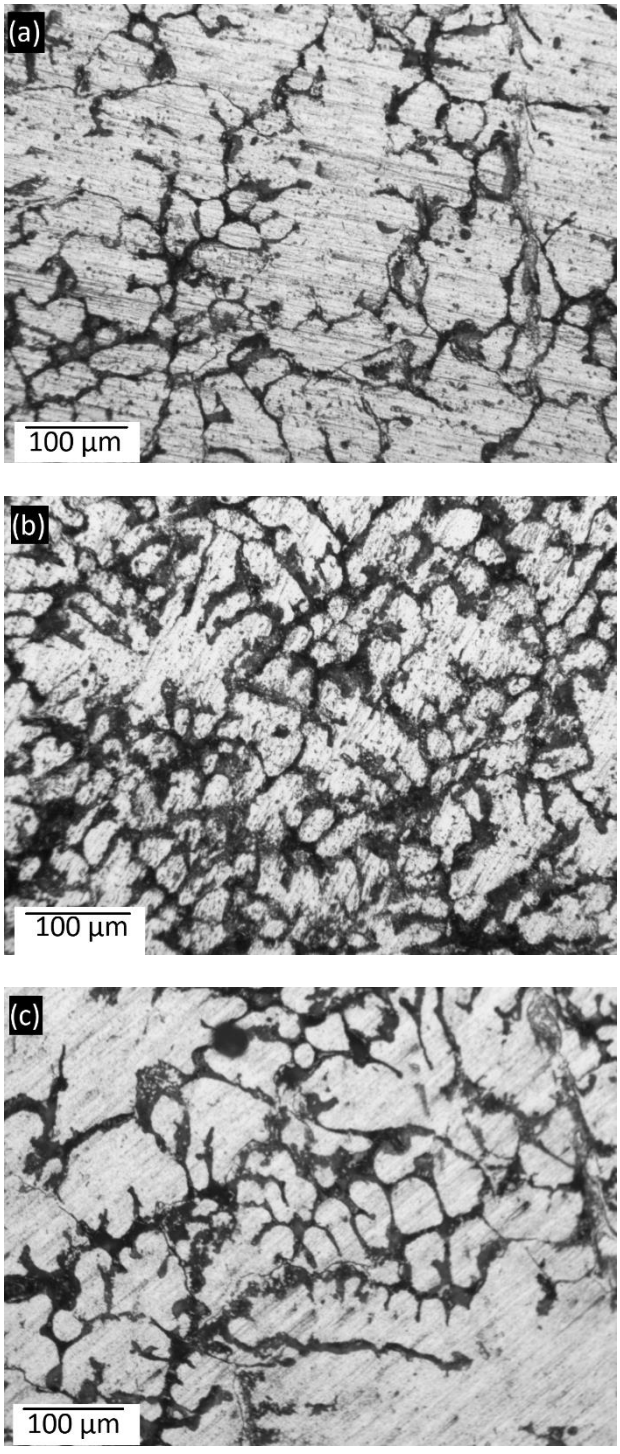

Fig. 2. Microstructural analysis of a) AA6082 alloy and hybrid composites, b) AA6082/3%BN/4%B_4C, c) AA6082/3%BN/4%B_4C/2%CCA, d) AA6082/3%BN/4%B_4C/4%CCA, e) AA6082/3%BN/4%B_4C/ 6%CCA.

3.2 Hardness of the AMMCs

Bulk hardness of all these five cast samples were measured and compared using Brinell hardness tester as shown in Fig. 3. During testing, a ball indenter of ø5 mm is used to apply a load of 250 kgf against each test specimen for 20 seconds. The indentation formed over the test specimen by the intender is used to calculate the hardness value. AA6082 alloy showed the least value of hardness (54.9 BHN) compared to all the composites. This clearly indicates the significance of reinforcements in improving overall material strength. Rise in reinforcement proportion within Al matrix improves the strength. But this phenomenon still possesses a variable threshold, beyond which the material property starts degrading. This threshold value is significantly dependent over the type of reinforcements, their proportion, particle size, orientation, distribution etc [38]. Similar observations were reported by a researcher in his

study, where varied Graphene Nanoplatelet binary Particles (GNPs) in Al matrix along with fixed proportion of silicon nitride, effectively controls the mechanical performance of the composite. Addition of graphene beyond 0.1wt%, considerably reduced the hardness of Al-GNPs composites, due to the agglomeration tendency of GNPs [39]. Excessive particle presence causes higher porosity and lower hardness [40].

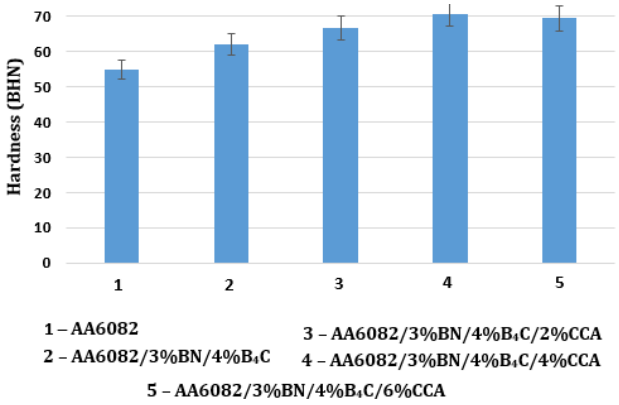

Fig. 3. Brinell hardness of AA6082 alloy and its hybrid composites.

Addition of BN and B_4C particles which is close to the density of aluminium matrix, resulted in effective distribution throughout the matrix and improvement of hardness by 13%. Further addition of CCA along with BN and B_4C resulted in improved grain refinement and dendritic particle distribution. Varied percentage of CCA (2, 4 and 6 wt.%) along with constant percentage of BN (3 wt.%) and B_4C (4 wt.%) revealed 21.8%, 28.7% and 26.4% improvement in hardness compared to alloy. The maximum hardness (70.7 BHN) was observed with 4 wt.% CCA, which reveals that presence of CCA beyond 4 wt.% causes clustering phenomenon and reduction of hardness. Wider dendritic spacing reduces the material strength as finer grain improves hardness [41]. This result was identified superior to similar studies conducted on hybrid composites like Al–Mg–Si /4%RHA/6%Al_2O_3 (64 BHN) and Al–Mg–Si/4%BLA/6%SiC (67 BHN) [42].

3.3 Impact strength of AMMC

Impact strength of all five cast samples were measured and compared using Izod impact tester as shown in Fig 4. AA6082 alloy showed the least value of impact strength (18 J) compared to all the composites. AA6082/3wt.%BN/4wt.%B_4C exhibited 11% improved impact strength compared to alloy. Presence of BN and B_4C resisted the crack propagation with their distribution and orientation across the matrix. The presence of reinforcements improves the notch toughness and composite strength [43]. Addition of CCA reduced the crack initiation sites and increased the amount of energy required for crack propagation. Varied percentage of CCA (2, 4 and 6 wt.%) along with constant percentage of BN (3 wt.%) and B_4C (4 wt.%) revealed 33.3%, 77.8% and 66.7% improvement in impact strength compared to alloy. Excessive presence of reinforcement particles beyond 10wt.% within the overall composition exhibited a slight decrement in impact strength. This is due to clustering phenomenon of dense ceramics that creates localized stress points and weakened certain zones with lack of particles, facilitating easy crack propagation [44].

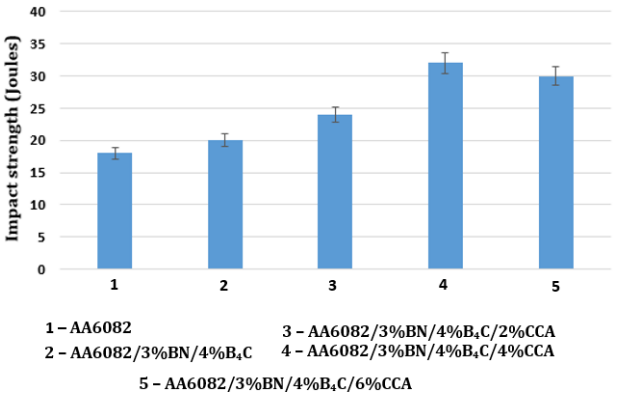

Fig. 4. Impact strength of AA6082 alloy and its hybrid composites.

3.4 SEM, EDX and elemental mapping analysis

In spite of the superior micro-hardness and impact strength, AA6082/3wt.%BN/4wt.%B_4C/4wt.%CCA hybrid composite was subjected to Field Emission Scanning Electron Microscope (FESEM) analysis as shown in Fig 5. It revealed good bondage of diverse reinforcements and effective distribution within the aluminium matrix. Minor voids are revealed due to the higher presence of diverse reinforcements. Voids act as nucleation sites for crack initiations [45]. However, no evidence of crack formations was revealed due to the presence of heterogeneous reinforcements, which have effectively resisted the crack initiation tendency.

Energy Dispersive X-Ray (EDX) Spectroscopy performed over AA6082/3wt.%BN/4wt.%B_4C/4wt.%CCA hybrid composite confirmed the elemental presence as shown in Fig 6. Highest peak of Al indicated matrix element and peaks of

B, C and N indicated the presence of reinforcements. Taller peak of O confirms the presence of CCA, where oxides of Si, Fe, K, Ca etc., forms the major composition.

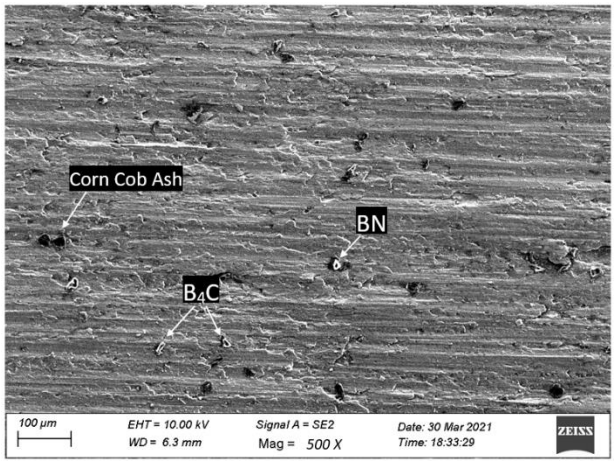

Fig. 5. SEM image of AA6082/3wt.%BN/4wt.%B_4C/4wt.%CCA hybrid composite.

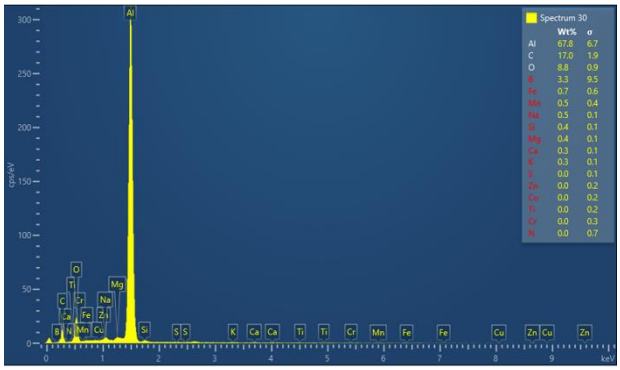

Fig. 6. EDX analysis of AA6082/3wt.%BN/4wt.%B_4C/4wt.%CCA composite.

Elemental mapping (Fig. 7) confirms the presence of compositional elements of AA6082/3wt.%BN/4wt.%B_4C/4wt.%CCA hybrid composite. Distribution of each component within the matrix is represented with different color code. This reveals an even distribution of reinforcements with minimal clustering tendency. FESEM results clearly highlights the distribution of B, Si and O which forms a major composition of reinforcements.

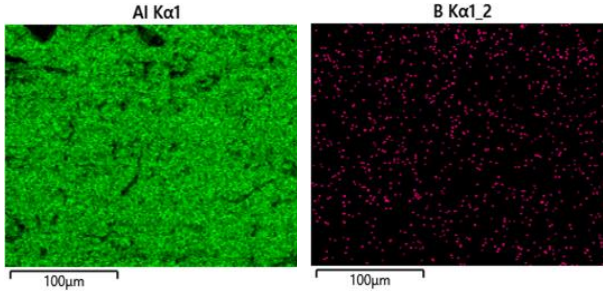

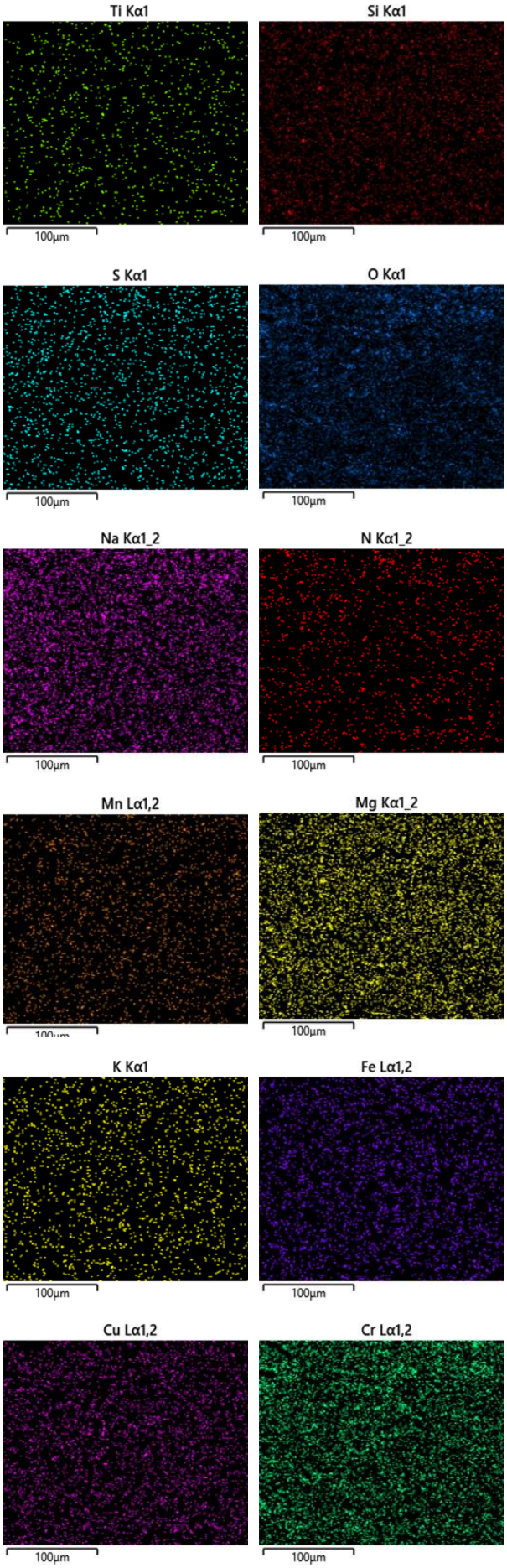

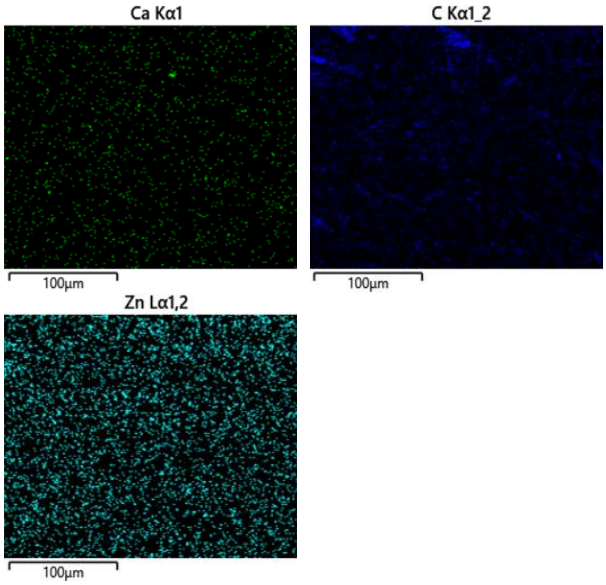

Fig. 7. Elemental mapping of AA6082/3wt.%BN/ 4wt.%B_4C/4wt.%CCA composite.

3.5 Wear behavior

Considering the superior mechanical performance, AA6082/3wt.%BN/4wt.%B_4C/4wt.%CCA hybrid composite was subjected for tribology analysis. Effect of input factors like applied load, sliding velocity and sliding distance on wear response were studied. Rate of wear being the chosen wear response, was effectively analyzed using Taguchi L_{27} array in Minitab software [46]. These three input parameters – load, velocity and distance were varied over a range of 10-25 N, 1-3 m/s and 750-1750 m respectively [47-50]. Unique combinations of 27 experimental trials were conducted to study their influence of wear response as shown in Table 3. Orthogonal array limits the number of experimental trials.

L_{27} orthogonal array is the most appropriate experiment plan, while considering variable interactions [51]. Taguchi approach was used for optimizing the large number of trials with an optimal design where complex structure of multi-factor combination is involved [52]. The contribution of each input factors and their interactions on tribo-responses are statistically analyzed using Analysis of Variance (ANOVA). Taguchi method uses both average as well as variance while utilizing the Signal-to-Noise (S/N) ratio [53]. S/N ratio helps in ranking these input factors based on their influence over wear response. Table 4. shows the result of ANOVA analysis for wear rate with confidence interval of 95% and significance level of 5%. The parameters that affect the wear rate, considered to possess a P-value less than 0.05. From the results, it is concluded that rate of wear is mainly affected by load with the highest percentage of influence at 51.6% followed by sliding distance at 26.4% and velocity at 12.6%.

Table 3. Wear behavior of the AA6082/3wt.%BN/ 4wt.%B_4C/4wt.%CCA composite.

Sl. No.	Load (N)	Velocity (m/s)	Distance (m)	Specific Wear rate ($\times 10^{-5}$) (mm^3/Nm)
1	15	1	750	$0.332 \cdot 10^{-5}$
2	15	2	750	$0.336 \cdot 10^{-5}$
3	15	3	750	$0.336 \cdot 10^{-5}$
4	15	1	1250	$5.84 \cdot 10^{-5}$
5	15	2	1250	$5.84 \cdot 10^{-5}$
6	15	3	1250	$6.253 \cdot 10^{-5}$
7	15	1	1750	$6.158 \cdot 10^{-5}$
8	15	2	1750	$6.163 \cdot 10^{-5}$
9	15	3	1750	$6.178 \cdot 10^{-5}$
10	25	1	1250	$3.965 \cdot 10^{-5}$
11	25	2	1250	$3.975 \cdot 10^{-5}$
12	25	3	1250	$3.985 \cdot 10^{-5}$
13	25	1	1750	$4.236 \cdot 10^{-5}$
14	25	2	1750	$4.259 \cdot 10^{-5}$
15	25	3	1750	$4.286 \cdot 10^{-5}$
16	25	1	750	$3.826 \cdot 10^{-5}$
17	25	2	750	$3.908 \cdot 10^{-5}$
18	25	3	750	$3.928 \cdot 10^{-5}$
19	35	1	1750	$3.901 \cdot 10^{-5}$
20	35	2	1750	$3.911 \cdot 10^{-5}$
21	35	3	1750	$3.915 \cdot 10^{-5}$
22	35	1	750	$3.122 \cdot 10^{-5}$
23	35	2	750	$3.141 \cdot 10^{-5}$
24	35	3	750	$3.142 \cdot 10^{-5}$
25	35	1	1250	$3.408 \cdot 10^{-5}$
26	35	2	1250	$3.457 \cdot 10^{-5}$
27	35	3	1250	$3.794 \cdot 10^{-5}$

Note: DF – Degrees of Freedom, Adj SS – Adjusted Sum of Squares, Adj MS – Adjusted Mean of Squares, F value – Fischer's chart, P value – probability statistics.

The regression equation (equation 1) developed using Minitab software correlates the input parameters - applied load, sliding velocity and sliding distance against wear response - specific ware rate based on their significance.

$$\begin{aligned} Specific\ Wear\ Rate\ =\ & -0.200 + 0.0944 \times \\ & Load - 2.508 \times Velocity\ +\ 0.002056 \times \\ & Distance\ +\ 0.0341 \times Load \times Distance\ + \\ & 0.000060 \times\ Distance \times Velocity\ + \\ & 0.001129 \times Load \times Velocity \end{aligned} \quad (1)$$

Table 4. ANOVA for rate of wear.

Source	DF	Adj SS	Adj MS	F-Value	P-Value	P (%)
Load	2	191.180	95.5898	53.09	0.004	51.6
Velocity	2	40.375	20.1874	11.21	0.014	12.6
Distance	2	90.274	45.1369	25.07	0.002	26.4
Load·Distance	4	120.371	15.38	8.73	0.001	8.4
Distance·Velocity	4	74.684	9.13	6.43	0.000	4.2
Load·Velocity	4	82.364	11.36	7.12	0.001	5.3
Error	20	36.008	1.8004			4.4
Total	26	357.836				

Taguchi method is well known of producing a better graphic visualization to determine the optimum condition by calculating SN ratio. The percentage of contribution of each factor was determined using ANOVA. Taguchi method requires comparatively less data to find the optimum condition than Response Surface Methodology (RSM) [54]. Therefore, Taguchi method was preferred than RSM as the experimental run turns time saving and economic. Moreover, RSM is best preferred in certain conditions, where parametric interactions claim a major percentage of contribution on optimization of wear responses [55]. Grey relational analysis is another promising technique, attempted by several researchers to optimize the control parameters influencing multi-responses [56].

3.6 Effect of input parameters on wear behavior

Hierarchical classification of factors that affect the output or response was based on their significance of influence as shown in Table 5. This classification is made based on the corresponding delta values of S/N ratios. The width between the highest and lowest level S/N value of each input factor gives the respective delta value [57]. Response table of means (Table 6) identified highest ranking for load, highlighting it as the most influential factor followed with sliding distance and sliding velocity.

Table 5. Response table for S/N ratio.

Level	Load (N)	Velocity (m/s)	Distance (m)
1	-3.567	-3.523	-3.560
2	-3.336	-3.329	-3.327
3	-3.270	-3.321	-30287
Delta	0.298	0.201	0.273
Rank	1	3	2

Table 6. Response table for means.

Level	Load (N)	Velocity (m/s)	Distance (m)
1	2082.3	2034.3	2053.1
2	335.5	333.8	324.1
3	268.9	318.7	309.5
Delta	1813.5	1715.6	1743.6
Rank	1	3	2

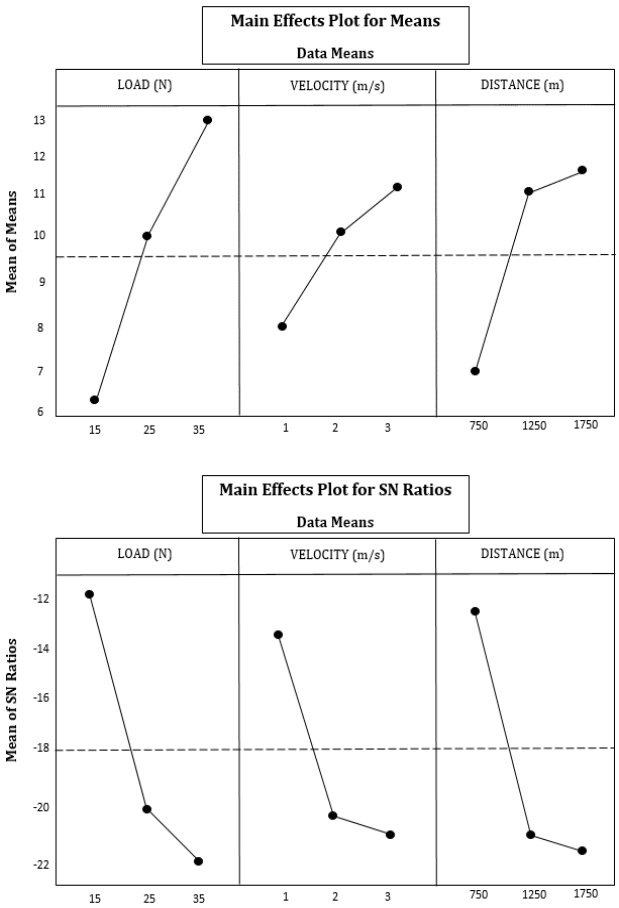

Fig. 8. a) Mean of means and b) Mean of S/N ratio plots for wear.

The mean of means plot (Fig. 8a) reveals the trend of wear rate against input parameters and mean of S/N ratios plot (Fig. 8b) identifies

the optimum combination of input parameters that produces minimum wear. For effective comparison, the input parameters – applied load, sliding velocity and sliding distance were varied at a range of 15-35 N, 1-3 m/s and 750-1750 m respectively. However, based on the existing literatures for similar application, the comparative analysis was conducted at extreme limits and mid-point of each parametric range [58-60]. This effectively reveals the rate of change in wear response against the input parameters. The highest S/N value of each input parameter is identified at an optimum combination of load – 15 N, sliding distance – 750 m and sliding velocity – 1 m/s.

Wear rate showed a proportional rise with increase in applied load from 15 to 35 N. Variation of wear rate is in accordance with Archard's law, where the load applied or pressure is directly proportional to volume of material removed [61]. The presence of hard reinforcements like BN, B_4C and oxides (SiO_2, Al_2O_3, MgO, FeO_3 and TiO_2) present in the CCA have also contributed significantly towards the improvement of mechanical and tribology performance [62]. Oxides present in CCA has effectively adhered the ceramics and improved wettability at the metal-ceramic interface.

At low load (15 N), shallow scratches and superficial craters are observed (Fig. 9a) predominantly indicating minor wear. This gradually transforms to form narrow grooves and exhibits gouging phenomenon at intermediate load (25 N) condition as seen in Fig 9b. Whereas, at high load (35 N), delamination phenomenon (Fig. 9c) indicates severe wear.

Wear rate showed a proportional rise with increase in sliding distance from 750 m to 1750 m. The slope showed a steep rise initially up to 1250 m, followed by a meagre slope until 1750 m. This trend was due to the accumulation of wear debris at the sliding interface where contributions from both the counter parts were involved. Higher oxide contributions from CCA along with C from B_4C together formed a tribolayer mixture along the sliding track affecting the sliding action with improper contact. This resulted in minimal wear.

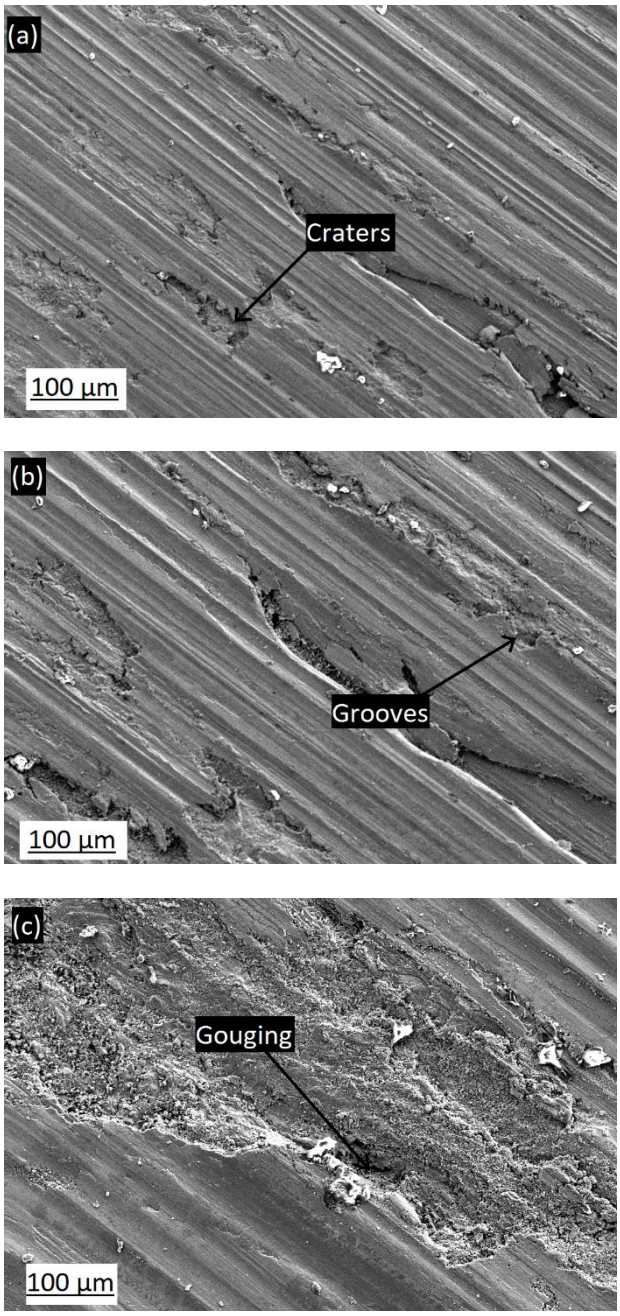

Fig. 9. Worn surface of AA6082/3wt.%BN/4wt.%B_4C/4wt.%CCA hybrid composite at constant sliding distance - 750 m, sliding velocity - 2 m/s with varied applied load a) 15 N, b) 25 N and c) 35 N.

At low distance (750 m), minor particle wreckage was observed as seen in Fig 10a. The depth of wear track was sufficient enough to reveal (Fig 10b) at intermediate distance (1250 m), which was effectively prevented at zones with hard ceramic presence. Whereas at high distance (1750 m) formation of mechanically mixed layer (MML) [63] was evident as seen in Fig 10c. This prevented effective rubbing along the interface causing reduced rate of material removal [64].

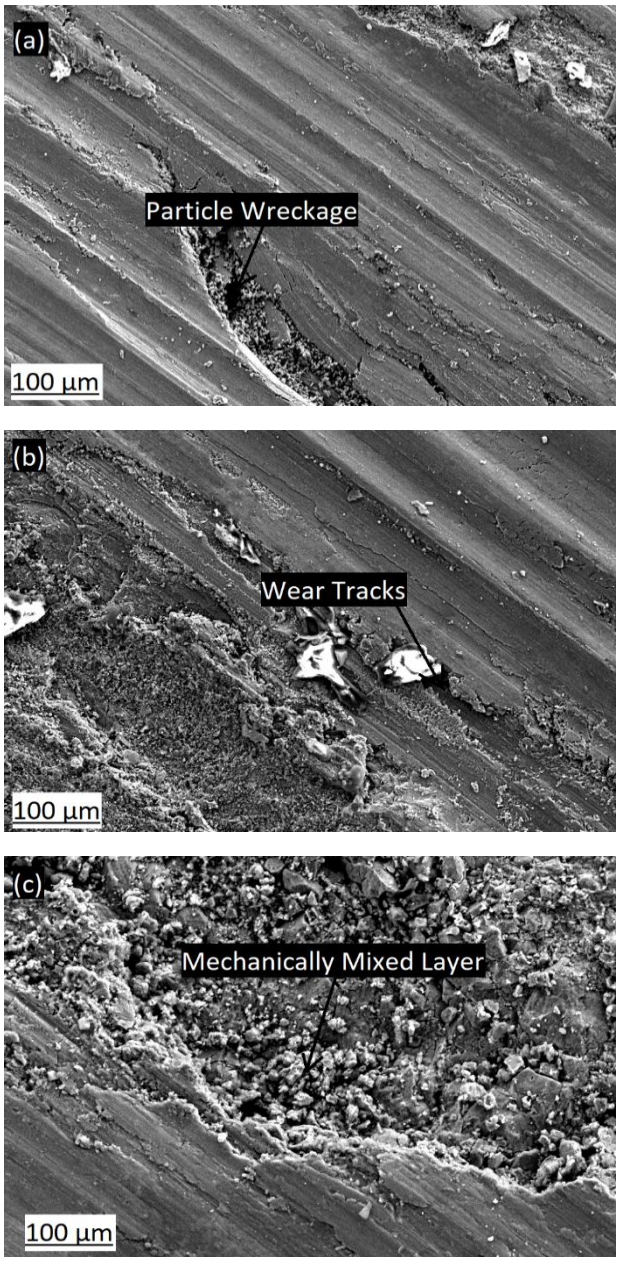

Fig. 10. Worn surface of AA6082/3wt.%BN/4wt.%B_4C/4wt.%CCA hybrid composite at constant applied load -25 N, sliding velocity - 1 m/s with varied sliding distance - a) 750 m, b) 1250 m and c) 1750 m.

Wear rate showed a proportional rise with varying sliding velocity (from 1.5 m/s to 3.5 m/s). The slope showed a steep rise initially up to 2.5 m/s, followed by a declining slope until 2.5 m/s. This trend was due to the layering of oxide layer over the sliding surface which reduces the interfacial contact beyond intermediate velocity (>2.5 m/s).

At low velocity (1.5 m/s), minimum particle pull outs and unstable debris are observed (Fig. 11a) along the sliding surface. At intermediate velocity (2.5 m/s), the contributions from both counter bodies increased and underwent oxidation to form a tribo-oxy layer [65] adhered to the sliding track. High oxide presence due to particle pull-outs triggered this phenomenon as seen in Fig. 11b. The asperities were not effective enough to scrap off this layer at high velocity (3.5 m/s) as seen in Fig. 11c. This thereby reduced the rate of material removal producing a declining slope of wear rate beyond 2.5 m/s.

SEM analysis at optimum wear condition (load - 15 N, sliding velocity – 1 m/s, sliding distance - 750 m) reveals (Fig. 12) minimal wear features like whisker scratches and minor cracks.

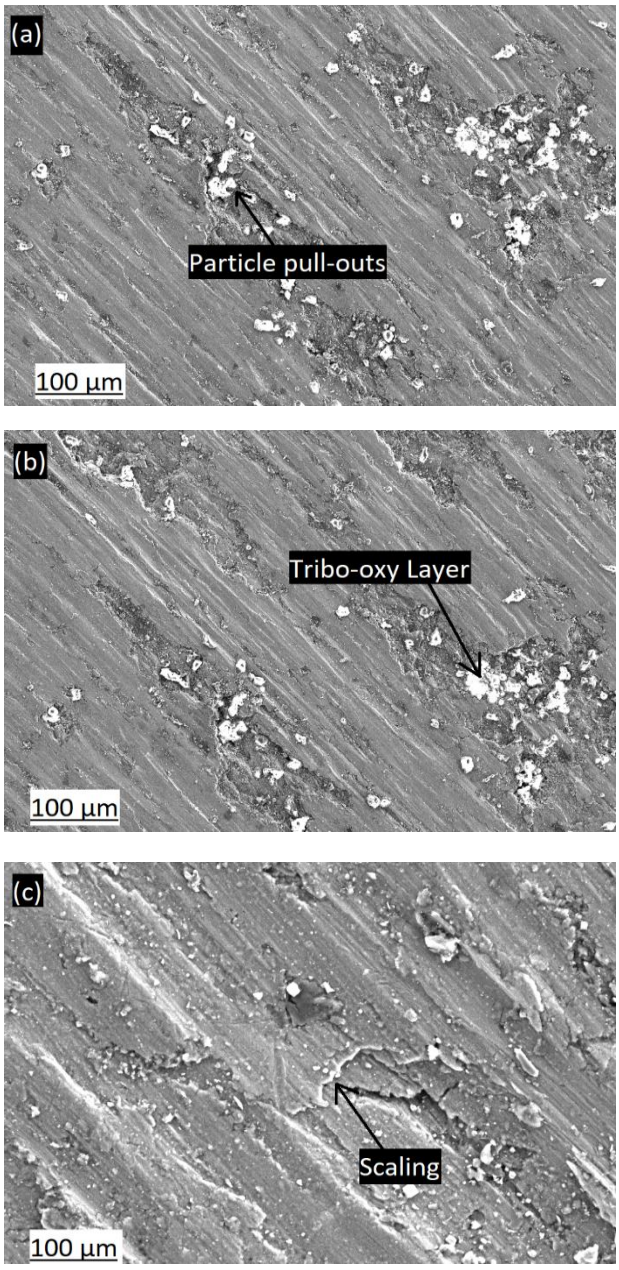

Fig. 11. Worn surface of AA6082/3wt.%BN/4wt.%B_4C/4wt.%CCA hybrid composite at constant sliding distance – 1250 m, applied load – 15 N and varied sliding velocity - a) 1 m/s, b) 2 m/s and c) 3 m/s.

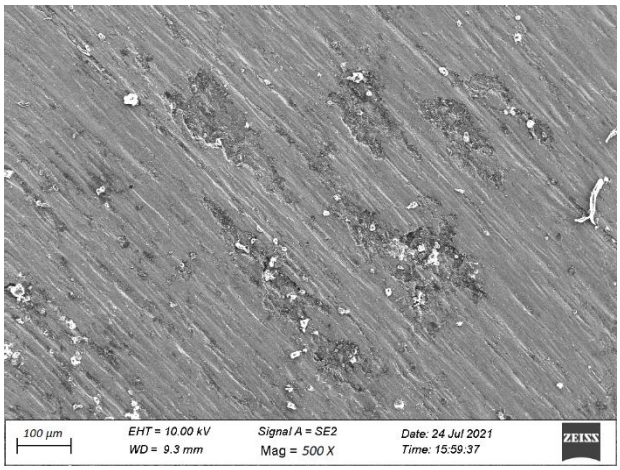

Fig. 12. Worn surface of AA6082/3wt.%BN/4wt.%B_4C/4wt.%CCA hybrid composite at optimum sliding condition-15 N, 1 m/s, 750 m.

The difference in predicted specific wear rate and experimentally obtained values were compared and validated at optimum wear condition (15 N, 1 m/s, 750 m). This reveals (Table 7) an acceptable error range of 2.1%.

Table 7. Validation of wear response at optimal wear condition.

Parameters	Observation
Response	Specific wear rate
Load (N)	15
Velocity (m/s)	1
Distance (m)	750
Predicted value (mm^3/Nm)	2.283×10-5
Experimental value (mm^3/Nm)	2.332×10-5
Error %	2.12

Similar to wear rate, COF is also a significant wear response which needs to be considered during tribology analysis. However, this study was primarily focused to study the influence of wear parameters on rate of wear. This was because there was no significant variation in COF observed with effect to load, distance and sliding velocity. Thus, this comparative analysis was limited to the influence of wear parameters on specific wear rate.

4. CONCLUSION

1. AA6082 alloy and AA6082/3wt.%BN/4wt.%B_4C hybrid composite was fabricated using stir casting technique. Corn cob ash was introduced as a tertiary reinforcement varied at 2, 4, 6wt.%, keeping 3wt.%BN and 4wt.%B_4C as constant during stir casting.
2. Homogeneous distribution and better grain refinement were observed with 4 wt.% CCA and clustering phenomenon with larger dendritic spacing was observed with higher wt.% (>4 wt.%) of CCA.
3. AA6082/3wt.%BN/4wt.%B_4C/4wt.%CCA hybrid composite revealed superior hardness (28.7%) and impact strength (77.8%) in comparison to the base alloy.
4. Experimental tribology analysis and S/N ratios based on Taguchi L_{27} orthogonal array reported least rate of wear at an optimum combination of input parameters - Load 15 N, Sliding distance 750 m and Sliding velocity 1 m/s.
5. Inference from the ANOVA identified load (51.6%) as the most influence parameter followed by sliding distance and sliding velocity.
6. All three input parameters defined a direct relationship towards the wear response at all combinations, and formation of tribolayer has suppressed this phenomenon at high sliding distance and high sliding velocity.
7. Formation of MML and oxide layers were identified as the predominant wear feature at higher sliding distance (>1250 m) and sliding velocity (>2.5 m/s), which controlled the rate of wear.

REFERENCES

[1] S.J.S. Chelladurai, S. Senthil Kumar, N. Venugopal, A. Pratip, T.C. Manjunath, S. Gnanasekaran, *A Review on Mechanical Properties and Wear Behavior of Aluminum Based Metal Matrix Composites*, Materials Today: Proceedings, vol. 37, pp. 908-916, 2020, doi: 10.1016/j.matpr.2020.06.053

[2] A. Moosa, A.Y. Awad, *Influence of Rice Husk Ash-Yttrium Oxide Addition on the Mechanical Properties Behavior of Aluminum Alloy Matrix Hybrid Composites*, International Journal of Current Engineering and Technology, vol. 6, no. 3, pp. 804-812, 2016.

[3] C.S. Jawalkara, Suman Kanta, N. Panwarb, M.D. Sharmab, H.S. Palib, *Effect of Particle Size Variation of Bagasse Ash on Mechanical Properties of Aluminum Hybrid Metal Matrix Composites*, Materials Today: Proceedings, vol. 21, pp. 2024-2029, 2020, doi: 10.1016/j.matpr.2020.01.319

[4] A. Shanmugasundaram, A. Sanjivi, R. Sellamuthu, *Study on the Effect of GTA Surface Melting and SiC Reinforcement on the Hardness, Wear and*

Corrosion Properties of AA 5086, Materials Today: Proceedings, vol. 5, iss. 2, pp. 6597-6606, 2018, doi: 10.1016/j.matpr.2017.11.315

[5] T.S. Kumar, R. Raghu, S. Shalini, *Hardness and Wear Behavior of Al 6061/ZrC Composite Processed by Friction Stir Processing*, Tribology in Industry, vol. 42, no. 4, pp. 582-591, 2020, doi: 10.24874/ti.855.02.20.10

[6] K.L. Pickering, M.G. Aruan, T.M. Le, *A Review of Recent Developments in Natural Fiber Composites and their Mechanical Performance*, Composites Part A: Applied Science and Manufacturing, vol. 83, pp. 98-112, 2016, doi: 10.1016/j.compositesa.2015.08.038

[7] R. Butola, A. Malhotra, M. Yadav, R. Singari, Q. Murtaza, P. Chandra, *Experimental Studies on Mechanical Properties of Metal Matrix Composites Reinforced with Natural Fibres Ashes*, SAE Technical Paper, no. 2019-01-1123, 2019, doi: 10.4271/2019-01-1123

[8] R. Butola, S. Kanwar, L. Tyagi, R.M. Singari, M. Tyagi, *Optimizing the Machining Variables in CNC Turning of Aluminum Based Hybrid Metal Matrix Composites*, SN Applied Sciences, vol. 2, iss. 8, pp. 1-9, 2020, doi: 10.1007/s42452-020-3155-8

[9] B. Subramaniam, B. Natarajan, B. Kaliyaperumal, S.J.S. Chelladurai, *Wear Behavior of Aluminum 7075—Boron Carbide-Coconut Shell Fly Ash Reinforced Hybrid Metal Matrix Composites*, Materials Research Express, vol. 6, no. 10, pp. 1065d3, 2019, doi: 10.1088/2053-1591/ab4052

[10] Y. He, H. Xu, B. Jiang, Z. Ji, M. Hu, *Microstructure, Mechanical and Tribological Properties of (APC+ B_4C)/Al Hybrid Composites Prepared by Hydrothermal Carbonized Deposition on Chips*, Journal of Alloys and Compounds, vol. 888, Available online, 2021, doi: 10.1016/j.jallcom.2021.161578

[11] K.K. Alaneme, T.M. Adewale, P.A. Olubambi, *Corrosion and Wear Behavior of Al–Mg–Si Alloy Matrix Hybrid Composites Reinforced with Rice Husk Ash and Silicon Carbide*, Journal of Materials Research and Technology, vol. 3, iss. 1, pp. 9-16, 2014, doi: 10.1016/j.jmrt.2013.10.008

[12] B. Subramaniam, B. Natarajan, B. Kaliyaperumal, S.J.S. Chelladurai, *Investigation on Mechanical Properties of Aluminium 7075 - Boron Carbide - Coconut Shell Fly Ash Reinforced Hybrid Metal Matrix Composites*, China Foundry, vol. 15, iss. 6, pp. 449-456, 2018, doi: 10.1007/s41230-018-8105-3

[13] T. Pratheep, S.J. Kishore, P.C, Theja, P. Punna, *Development And Wear Behavior Investigation on Aluminum-7075/B_4C/Fly Ash Metal Matrix Composites*, Advanced Composites and Hybrid Materials, vol. 3, iss. 1, pp. 255-265, 2020, doi: 10.1007/s42114-020-00145-5

[14] O.B. Fatile, J.I. Akinruli, A.A. Amori, *Microstructure and Mechanical Behaviour of Stir-Cast Al-Mg-Si Alloy Matrix Hybrid Composite Reinforced with Corn Cob Ash and Silicon Carbide*, International Journal of Engineering and Technology Innovation, vol. 4, no. 4, pp. 251-259, 2014.

[15] K.R. Garadimani, G. Raju, K. Kodancha, *Study on Mechanical Properties of Corn Cob Particle and E-Glass Fiber Reinforced Hybrid Polymer Composites*, American Journal of Materials Science, vol. 5, no. 3C, pp. 86-91, 2015.

[16] S.C. Prasanna, C. Ramesh, R. Manivel, A. Manikandan, *Preparation of Al6061-SiC with Neem Leaf Ash in AMMC's by Using Stir Casting Method and Evaluation of Mechanical, Wear Properties and Investigation on Microstructures*, Applied Mechanics and Materials, vol. 854, pp. 115-120, 2016, doi: 10.4028/www.scientific.net/AMM.854.115

[17] S.P. Singh, K.A.V. Geethan, D. Elilraja, T. Prabhuram, J.I. Durairaj, *Optimization of Dry Sliding Wear Performance of Functionally Graded Al6061/20% SiC Metal Matrix Composite using Taguchi Method*, Materials Today: Proceedings, vol. 22, pp. 2824-2831, 2020, doi: 10.1016/j.matpr.2020.03.414

[18] K.K. Ekka, S.R. Chauhan, *Dry Sliding Wear Characteristics of SiC and Al_2O_3 Nanoparticulate Aluminium Matrix Composite Using Taguchi Technique*, Arabian Journal for Science and Engineering, vol. 40, iss. 1, pp. 571-581, 2015, doi: 10.1007/s13369-014-1528-2

[19] M.C. Şenel, M. Gürbüz, *Investigation on Mechanical Properties and Microstructure of B_4C/Graphene Binary Particles Reinforced Aluminum Hybrid Composites*, Metals and Materials International, vol. 27, iss. 7, pp. 2438-2449, 2021, doi: 10.1007/s12540-019-00592-w

[20] P.K. Gupta, M.K. Gupta, *Mechanical and Microstructural Analysis of Al-Al_2O_3/B_4C Hybrid Composites*, Proceedings of the Institution of Mechanical Engineers, Part L: Journal of Materials: Design and Applications, vol. 234, iss. 12, pp. 1503-1514, 2020, doi: 10.1177/1464420720942554

[21] B.U. Odoni, F.O. Edoziuno, C.C. Nwaeju, R.O. Akaluzia, *Experimental Analysis, Predictive Modelling and Optimization of Some Physical and Mechanical Properties of Aluminium 6063 Alloy Based Composites Reinforced with Corn Cob Ash*, Journal of Materials and Engineering Structures, vol. 7, no. 3, pp. 451-465, 2020.

[22] T. Opel, N. Langhof, W. Krenkel, *Development and Tribological Studies of a Novel Metal-Ceramic Hybrid Brake Disc*, International Journal of

Applied Ceramic Technology, vol. 19, iss.1, pp. 1-13, 2021, doi: 10.1111/ijac.13826

[23] K.O. Babaremu, O.O. Joseph, *Experimental Study of Corncob and Cow horn AA6063 Reinforced Composite for Improved Electrical Conductivity*, International Conference on Engineering for Sustainable World, vol. 1378, iss. 4, pp. 1-9, 2019, doi: 10.1088/1742-6596/1378/4/042048

[24] S.M.L. Nai, M. Gupta, C.Y.H. Lim, *Synthesis and Wear Characterization of Al based, Free Standing Functionally Graded Materials: Effects of Different Matrix Compositions*, Composite Science and Technology, vol. 63, iss. 13, pp. 1895–1909, 2003, doi: 10.1016/S0266-3538(03)00158-1

[25] S.Y. Pawar, Y.R. Kharde, *Effect of Dual Reinforced Ceramic Particles on Elevated Temperature Tribological Properties of Hybrid Aluminium Matrix Composites*, Advances in Materials and Processing Technologies, pp. 1-17, 2021, doi: 10.1080/2374068X.2020.1853495

[26] P.R. Jadhav, B.R. Sridhar, M. Nagaral, J.I. Harti, *Evaluation of Mechanical Properties of B_4C and Graphite Particulates Reinforced A356 Alloy Hybrid Composites*, Materials Today: Proceedings, vol. 4, iss. 9, pp.9972-9976, 2017, doi: 10.1016/j.matpr.2017.06.304

[27] N. Ramadoss, K. Pazhanivel, G. Anbuchezhiyan, *Synthesis of B_4C and BN Reinforced Al7075 Hybrid Composites using Stir Casting Method*, Journal of Materials Research and Technology, vol. 9, iss. 3, pp. 6297-6304, 2020, doi: 10.1016/j.jmrt.2020.03.043

[28] K. Srivallirani, M.V. Rao, *Fabrication and Mechanical Characterization of Al 7050/TiO_2/BN Hybrid Metal Matrix Composites*, Materials Today: Proceedings, vol. 39, pp. 1750-1753, 2021, doi: 10.1016/j.matpr.2020.06.386

[29] M. Azadi, M. Zolfaghari, S. Rezanezhad, M. Azadi, *Effects of SiO_2 Nano-Particles On Tribological and Mechanical Properties of Aluminum Matrix Composites by Different Dispersion Methods*, Applied Physics A, vol. 124, iss. 5, pp. 1-3, 2018, doi: 10.1007/s00339-018-1797-9

[30] M.K. Sahu, R.K. Sahu, *Fabrication of Aluminum Matrix Composites by Stir Casting Technique and Stirring Process Parameters Optimization*, in T. Vijayaram (Ed.): Advanced Casting Technologies, IntechOpen, pp. 111-123, 2018, doi: 10.5772/intechopen.73485

[31] B.V. Ramnath, C. Elanchezhian, M. Jaivignesh, S. Rajesh, C. Parswajinan, A. Siddique Ahmed Ghias, *Evaluation of Mechanical Properties of Aluminium Alloy-Alumina-Boron Carbide Metal Matrix Composites*, Materials & Design, vol. 58, pp. 332-338, 2014, doi: 10.1016/j.matdes.2014.01.068

[32] S.C. Tjong, K.C. Lau, S.Q. Wu, *Wear of Al-based Hybrid Composites Containing BN and SiC Particulates*, Metallurgical and Materials Transactions A, vol. 30, iss. 9, pp. 2551-2555, 1999, doi: 10.1007/s11661-999-0265-8

[33] N.A. Latif, N.F. Mohd Joharudin, M.S. Mustapa, S.W. Hao, A. Supawi, N.Z. Hassan, Z. Noranai, *Crystalline Rice Husk Silica Reinforced AA7075 Aluminium Chips by Cold Compaction Method*, Materialwissenschaft und Werkstofftechnik, vol. 52, iss. 10, pp. 1121-1128, 2021, doi: 10.1002/mawe.202000319

[34] M.K. Sahu, R.K. Sahu, *Optimization of Stirring Parameters using CFD Simulations for HAMCs Synthesis by Stir Casting Process*, Transactions of the Indian Institute of Metals, vol. 70, iss. 10, pp. 2563-2570, 2017, doi: 10.1007/s12666-017-1119-5

[35] M.K. Sahu, R.K. Sahu, *Synthesis, Microstructure and Hardness of Al 7075/B_4C/Fly-Ash Composite using Stir Casting Method*, Materials Today: Proceedings, vol. 27, pp. 2401-2406, 2020, doi: 10.1016/j.matpr.2019.09.150

[36] R. Butola, L. Tyagi, L. Kem, M.S. Ranganath, Q. Murtaza, *Mechanical and Wear Properties of Aluminium Alloy Composites: A Review*, Manufacturing Engineering, vol. 9, iss. 1, pp. 369-391, 2020, doi: 10.1007/978-981-15-4619-8_28

[37] HH. Kalaa, K.K.S. Merb, S. Kumar, *A Review on Mechanical and Tribological Behaviors of Stir Cast Aluminum Matrix Composites*, Procedia Materials Science, vol. 6, pp. 1951-1960, 2014, doi: 10.1016/j.mspro.2014.07.229

[38] M. Gurbuz, T. Mutuk, *Effect of Process Parameters on Hardness and Microstructure of Graphene Reinforced Titanium Composites*, Journal of Composite Materials, vol. 52, iss. 4, pp. 543–551, 2018, doi: 10.1177/0021998317745143

[39] M. Gurbuz, M.C. Senel, E. Koc, *The Effect of Sintering Temperature, Time and Graphene Addition on the Mechanical Properties and Microstructure of Aluminum Composites*, Journal of Composite Materials, vol. 52, iss. 4, pp. 553-563, 2018, doi: 10.1177/0021998317740200

[40] M.C. Senel, M. Gurbuz, E. Koc, *Fabrication and characterization of SiC and Si_3N_4 Aluminum Matrix Composites*, Universal Journal of Materials Science, vol. 5, no. 4, pp. 95-101, doi: 10.13189/ujms.2017.050403

[41] N. Idusuyi, P.O. Oviroh, A.H. Adekoya, *A Study on the Corrosion and Mechanical Properties of an Al6063 Reinforced with Egg Shell Ash and Rice Husk Ash*, International Mechanical Engineering Congress and Exposition, vol. 12, 2018, doi: 10.1115/IMECE2018-86662

[42] M.K. Sahu, R.K. Sahu, *Aluminum Based Hybrid Metal Matrix Composites: A Review of Selection Philosophy and Mechanical Properties for Advanced Applications*, International Journal of Mechanical and Production Engineering Research and Development, vol. 10, pp. 8-28, 2020.

[43] R. Butola, C. Pratap, A. Shukla, R.S. Walia, *Effect on the Mechanical Properties of Aluminum-based Hybrid Metal Matrix Composite using Stir Casting Method*, In Materials Science Forum, vol. 969, pp. 253-259, 2019, doi: 10.4028/www.scientifc.net/msf.969.253

[44] D.W. Wong, L. Lin, P.T. McGrail, T. Peijs, P.J. Hogg, *Improved Fracture Toughness of Carbon Fibre/Epoxy Composite Laminates using Dissolvable Thermoplastic Fibres*, Composites Part A: Applied Science and Manufacturing, vol. 41, iss. 6, pp. 759-767, 2010, doi: 10.1016/j.compositesa.2010.02.008

[45] S. Gangwar, P. Arya, V.K. Pathak, *Optimal Material Selection for Ship Body Based on Fabricated Zirconium Dioxide/ Silicon Carbide Filled Aluminium Hybrid Metal Alloy Composites Using Novel Fuzzy Based Preference Selection Index*, Silicon, vol. 13, iss. 8, pp. 2545-2562, 2021, doi: 10.1007/s12633-020-00600-4

[46] A. Saravanakumar, L. Rajeshkumar, D. Balaji, M.J. Karunan, *Prediction of Wear Characteristics of AA2219-Gr Matrix Composites using GRNN and Taguchi-based Approach*, Arabian Journal for Science and Engineering, vol. 45, iss. 11, pp. 9549-9457, 2020, doi: 10.1007/s13369-020-04817-8

[47] R. Nithesh, N. Radhika, S. Shiam Sunder, *Mechanical Properties and Adhesive Scuffing Wear Behavior of Stir Cast Cu–Sn–Ni/Si_3N_4 Composites*, Journal of Tribology, vol. 139, no. 6, pp. 061603-06112, 2017, doi: 10.1115/1.4036185

[48] R.A. Khosroshahi, N. Nemati, M. Emamy, N. Parvini, A. Zolriasatein, *Investigation of Wear Properties of Al-4.5 wt.% Cu Nano-Composite Reinforced with Different Weight Percent of TiC Nano Particles Produced by Mechanical Alloying*, In Advanced Materials Research, vol. 545, pp. 124-128, 2012, doi: 10.4028/www.scientific.net/AMR.545.124

[49] C.M. Athev, J.N. Alistar, N. Radhika, *Synthesis of Al LM25/TiC Composite Using Squeeze Casting Method and Investigation of its Mechanical and Adhesive Wear Properties*, Materials Today: Proceedings, vol. 5, iss. 5, pp. 12681-12692, 2018, doi: 10.1016/j.matpr.2018.02.252

[50] A.P. Reddy, P.V. Krishna, R.N. Rao, *Dry Sliding Wear Behaviour of Ultrasonically-Processed AA6061/SiCp Nanocomposites*, International Journal of Automotive and Mechanical Engineering, vol. 14, iss. 4, pp. 4747-4758, 2017, doi: 10.15282/ijame.14.4.2017.12.0373

[51] J. Sudeepan, K. Kumar, T.K. Barman, P. Sahoo, *Study of Friction and Wear of ABS/ZnO Polymer Composite using Taguchi Technique*, Procedia Materials Science, vol. 6, pp. 391-400, 2014, doi: 10.1016/j.mspro.2014.07.050

[52] W.H. Chen, J.S. Wang, M.H. Chang, J.K. Mutuku, A.T. Hoang, *Efficiency Improvement Of A Vertical-Axis Wind Turbine Using a Deflector Optimized by Taguchi Approach with Modified Additive Method*, Energy Conversion and Management, vol. 245, pp. 114609-114626, 2021, doi: 10.1016/j.enconman.2021.114609

[53] A. Pattanaik, M.P. Satpathy, S.C. Mishra, *Dry Sliding Wear Behavior of Epoxy Fly Ash Composite with Taguchi Optimization*, Engineering Science and Technology, an International Journal, vol. 19, iss. 2, pp. 710-716, 2016, doi: 10.1016/j.jestch.2015.11.010

[54] M.S. Said, J.A. Ghani, M.S. Kassim, S.H. Tomadi, C.H. Haron, *Comparison between taguchi method and response surface methodology (RSM) in optimizing machining condition*, In Proceeding of 1st International Conference on Robust Quality Engineering, 2013, pp. 60-68.

[55] M.K. Sahu, R.K. Sahu, *Experimental Investigation, Modeling, and Optimization of Wear Parameters of B_4C and Fly-Ash Reinforced Aluminum Hybrid Composite*, Frontiers in Physics, vol. 8, pp. 219, 2020, doi: 10.3389/fphy.2020.00219

[56] M.K. Sahu, A. Valarmathi, S. Baskaran, V. Anandakrishnan, R.K. Pandey, *Multi-Objective Optimization of Upsetting Parameters of Al–TiC Metal Matrix Composites: A Grey Taguchi Approach*, Proceedings of the Institution of Mechanical Engineers, Part B: Journal of Engineering Manufacture, vol. 228, iss. 11, pp. 1501-1507, 2014, doi/abs/10.1177/0954405413519434

[57] R. Krishna Kumar, N. Radhika, Manu Sam, *Synthesis of Aluminum Composites Using Squeeze Casting and Investigating the Effect of Reinforcements on their Mechanical and Wear Properties*, Transactions of the Indian Institute of Metals, vol. 72, pp. 2299-2310, 2019, doi: 10.1007/s12666-019-01680-6

[58] A. Coyal, N. Yuvaraj, R. Butola, L. Tyagi, *An Experimental Analysis of Tensile, Hardness and Wear Properties of Aluminium Metal Matrix Composite through Stir Casting Process*, SN Applied Sciences, vol. 2, iss. 5, pp. 1-10, 2020, doi: 10.1007/s42452-020-2657-8

[59] L. Tyagi, R. Butola, A.K. Jha, *Mechanical and Tribological Properties of AA7075-T6 Metal Matrix Composite Reinforced with Ceramic Particles and Aloevera Ash via Friction Stir Processing*, Materials

Research Express, vol. 7, no. 6, pp. 1-14, 2020, doi: 10.1088/2053-1591/ab9c5e

[60] N. Radhika, A. Vaishnavi, G.K. Chandran, *Optimisation of Dry Sliding Wear Process Parameters for Aluminium Hybrid Metal Matrix Composites*, Tribology in Industry, vol. 36, no. 2, 2014.

[61] G. Dirisenapu, L. Dumpala, S. Pichi Reddy, *The Influence of B_4C and BN Nanoparticles on Al 7010 Hybrid Metal Matrix Nanocomposites*, Emerging Materials Research, vol. 9, iss. 3, pp. 558-563, 2020, doi: 10.1680/jemmr.19.00080

[62] M. Sam, N. Radhika, *Influence of Carbide Ceramic Reinforcements in Improving Tribological Properties of A333 Graded Hybrid Composites*, Defence Technology, In Press, 2021, doi: 10.1016/j.dt.2021.06.005

[63] B. Venkataraman, G. Sundararajan, *Correlation between the Characteristics of the Mechanically Mixed Layer and Wear Behaviour of Aluminium, Al-7075 Alloy and Al-MMCs*, Wear, vol. 245, iss. 1-2, pp. 22-38, 2000, doi: 10.1016/S0043-1648(00)00463-4

[64] M. Sam, R. Jojith, N. Radhika, *Progression in Manufacturing of Functionally Graded Materials and Impact of Thermal Treatment—A Critical Review*, Journal of Manufacturing Processes, vol. 68, pp. 1339-1377, 2021, doi: 10.1016/j.jmapro.2021.06.062

[65] D. Lu, M. Gu, Z. Shi, *Materials Transfer and Formation of Mechanically Mixed Layer in Dry Sliding Wear of Metal Matrix Composites against Steel*, Tribology Letters, vol. 6, pp. 57-61, 1999, doi: 10.1023/A:1019182817316